

## Durham Research Online

---

### Deposited in DRO:

07 November 2019

### Version of attached file:

Accepted Version

### Peer-review status of attached file:

Peer-reviewed

### Citation for published item:

Huang, Haozhong and Li, Zhongju and Teng, Wenwen and Huang, Rong and Liu, Qingsheng and Wang, Yaodong (2019) 'Effects of EGR rates on combustion and emission characteristics in a diesel engine with n-butanol/PODE3-4/diesel blends.', *Applied thermal engineering*, 146 . pp. 212-222.

### Further information on publisher's website:

<https://doi.org/10.1016/j.applthermaleng.2018.09.126>

### Publisher's copyright statement:

© 2019 This manuscript version is made available under the CC-BY-NC-ND 4.0 license  
<http://creativecommons.org/licenses/by-nc-nd/4.0/>

### Additional information:

---

### Use policy

The full-text may be used and/or reproduced, and given to third parties in any format or medium, without prior permission or charge, for personal research or study, educational, or not-for-profit purposes provided that:

- a full bibliographic reference is made to the original source
- a [link](#) is made to the metadata record in DRO
- the full-text is not changed in any way

The full-text must not be sold in any format or medium without the formal permission of the copyright holders.

Please consult the [full DRO policy](#) for further details.

1     **Effects of EGR rates on combustion and emission characteristics in**  
2     **a diesel engine with n-butanol/PODE<sub>3-4</sub>/diesel blends**

3

4     Haozhong Huang<sup>a\*</sup>, Zhongju Li<sup>a</sup>, Wenwen Teng<sup>a</sup>, Rong Huang<sup>a</sup>, Qingsheng Liu<sup>a</sup>,  
5     Yaodong Wang<sup>b</sup>

6         <sup>a</sup>*College of Mechanical Engineering, Guangxi University, Nanning 530004, China*

7         <sup>b</sup>*Sir Joseph Swan Institute for Energy Research, Newcastle University, Newcastle Upon Tyne, NE1 7RU,*  
8     *UK*

9     \*Corresponding author: Tel.:+86-771-3232294 mail: hhz421@gxu.edu.cn (H.  
10    Huang).

## Abstract

An experimental investigation is conducted on the influence of EGR (Exhaust Gas Recirculation) rates (0-40%) on the combustion and emission characteristics of n-butanol/diesel/PODE<sub>3-4</sub> blends at low-temperature combustion mode in diesel engine. The results show that at identical EGR rate, compared to D100 (diesel fuel), the peak values both of the mean cylinder pressure and the heat release rate of BD20 (20% butanol and 80% diesel in volume) are increased, ignition delay is extended, and the brake thermal efficiency is enhanced. Concerning BD20 blended with PODE<sub>3-4</sub>, the ignition delay is shortened, while both the brake thermal efficiency and the combustion efficiency increase. At the EGR rate below 30%, as the EGR rate grows, the effects on emission of soot, CO and HC are not significant, while the emission of NO<sub>x</sub> is sharply reduced; when the EGR rate is above 30%, as it grows, the emissions of soot, CO, and HC drastically rise. As EGR rate grows, the total particulate matter (PM) number concentrations of four fuels firstly decline and then rise, the total PM mass concentrations keep stable firstly and then rise drastically. As the proportion of added PODE<sub>3-4</sub> in BD20 grows, the particle geometric mean diameters further decrease.

*Keywords:* N-butanol/PODE<sub>3-4</sub>/diesel; EGR; low-temperature combustion; emission

## 1. Introduction

Diesel engines are widely applied in engineering machinery because their high compression ratio, high thermal efficiency, and excellent stability. However, the difficulty in simultaneous reduction of soot and NO<sub>x</sub> is a severe challenge for the survival of diesel engines. To meet the increasingly severe exhaust regulations, the interest of researchers in developing advanced combustion modes, including PCCI [1], RCCI [2], GCI [3], LTC [4] increased. As a promising advanced combustion mode, the great potential of LTC in addressing the trade-off between NO<sub>x</sub> and soot emissions has been proved in many studies.

In recent years, with aggravating energy consumption and challenging fuel consumption regulations, the attention is increasingly focused on exploring renewable clean alternative fuels, such as alcohols [5-7], ethers [8-10], esters [11-13], and natural gas [14,15]. As a renewable substitute for diesel, the n-butanol has drawn extensive interest owing to its prominent fuel properties [16-18] compared to ethanol and methanol. Produced from the biomass feedstock fermentation process, n-butanol is confirmed as a biomass-based renewable fuel [19-21]. Considering its high oxygen content, adding n-butanol to diesel has been proven to be effective in reducing harmful emissions, mainly the soot emissions [22]. Due to its higher latent heat, n-butanol has lower in-cylinder combustion temperature and reduced NO<sub>x</sub> emission than ethanol [23]. A decreasing trend in NO<sub>x</sub> and soot emissions was obtained with moderate EGR and high n-butanol proportion [24]. However, adding n-butanol with low cetane number and low heat value, to diesel, increases the maximum pressure rise rate (MPRR); moreover, the brake specific fuel consumption (BSFC) is also high [25, 26]. The increment in PAHs (polycyclic aromatic hydrocarbon) due to the increasing of n-butanol fraction was observed [27]. Thus, for further improving the performance and emissions of a diesel engine fueled with n-butanol/diesel blends and making it more suitable for diesel engine application, seeking a potential promising substitute for diesel or altering the fuel properties is essential.

Polyoxymethylene dimethyl ethers (PODE) is a potential renewable alternative biofuel with high cetane number, oxygen content, no C-C bond, and substantial soot reduction potential. PODE<sub>3-4</sub> with the number of CH<sub>2</sub>O unit between 3 and 4, obtained by synthesizing PODE<sub>2</sub>, PODE<sub>3</sub>, and PODE<sub>4</sub> with a mass distribution of 2.553%:88.9%:8.48% [28]. It has achieved mass production, so that PODE blend can be used in modern diesel engines [29]. Many investigations on PODE have been carried out, demonstrating it is a potential substitute for diesel. Adding PODE to pure diesel improves ignitability of fuel blends [30], shortens the combustion duration and enhances the combustion efficiency [31, 32]. A decreasing trend in MPRR was observed upon adding PODE<sub>3-4</sub> to butanol/diesel blends [33]. The trade-off relationship between thermal efficiency and engine noise was eliminated, and simultaneous reduction in PM and NO<sub>x</sub> with high efficiency was achieved under the multiple premixed compression ignition mode fueling gasoline/diesel/PODE blends [34]. Tong et al. [35] and Li et al. [36] obtained ultra-low smoke and NO<sub>x</sub> by using PODE as a substitute under advanced combustion mode. Liu et al. [37, 38] achieved soot-free combustion using PODE/diesel blends, and CO and HC emissions decreased dramatically at the expense of a slight increment in NO<sub>x</sub> emission. Huang et al. [39] carried out an experiment on a four-cylinder turbocharged diesel engine, proving that adding PODE to n-butanol/diesel blends led to a reduction in the total particle mass concentration and the accumulated particulate matter number concentration. In a nutshell, fuel design and advanced combustion concept are potential solutions for the high-efficiency and clean combustion.

The low-temperature combustion achieved by introducing a large proportion of EGR rate is a very effective measure to reduce the NO<sub>x</sub> emissions of diesel engines. Also, from the literature reviewed above, n-butanol and PODE have been intensively investigated as excellent potential biofuels for diesel. However, most of the available papers are focusing on the characteristic of combustion performance and the emissions of engines fueled with n-butanol/diesel blends and PODE/diesel blends. Only a few research focus on adding PODE to n-butanol/diesel blends for further

improving combustion and emissions characteristic; therefore, it is valuable to explore the effect of fueling strategies on LTC with n-butanol/PODE/diesel blends. This study evaluates the potential to achieve high efficiency with low harmful emissions, particulate emissions of a turbocharged engine with n-butanol/PODE/diesel blends over a wide range of EGR rates. The results may provide valuable insight on the effect of PODE on diesel particulate emissions and may prove to be effective in improving PM emissions characteristic.

## **2. Experimental facility and steps**

### **2.1. Research engine and device**

The experimental engine is a 4-cylinder, turbocharger (VGT) Light-duty vehicle diesel engine stocked with the common-rail fuel injection system. Table 1 lists the main parameters of the engine, while Fig. 1 shows the schematic diagram of the experimental apparatus.

Open-type of BOSCH ECU, ETAS INCA6.2, and Bosch second generation EFI system were used to adjust parameters such as injection pressure, timing, fuel mass, and multiple injections accurately. Additionally, the software (INCA) was used to adjust the EGR rate by altering the opening of the EGR valve. A Kistler 6052CU20 piezo-transducer installed on the cylinder top measured the heat release rate (HRR) and cylinder pressure rise rate; the data from the transducer was processed to obtain the heat release rate.

### **2.2. Emission measurement**

A Horiba MEXA7500DEGR measurement system measured the gaseous emission samples which include NO<sub>x</sub>, CO, HC, and CO<sub>2</sub>; an AVL 415S smoke meter analyzed the soot gas opacity. Based on the specifications of the Horiba, the quantity of NO<sub>x</sub> was measured using a chemiluminescent detector (CLD). CO was measured by a non-dispersive infrared analyzer (NDIR), and the HC amount was obtained using a flame ionization detector (FID). The CO<sub>2</sub> volume concentrations of the intake port and exhaust manifold were both measured to define the EGR rate.

The particle size distribution, number concentration, and particle mass concentration were measured using the fast particle analyzer DMS500, which showed that the particles number/size spectrum varied from 5 to 1000 nm.

### **2.3. Fuels**

In this study, four different types of fuels, i.e., pure diesel (D100), BD20, BDP10, and BDP20, were tested. Among them, the pure diesel was used as the primary reference fuel. BD20 was obtained by blending 20% n-butanol in diesel (v/v); BDP10 and BDP20 were prepared by blending 10% or 20% PODE<sub>3-4</sub> into BD20 (v/v), respectively. BDP20 was chosen because of the great mutual solubility of 20% PODE with BD20 at 20 °C. Table 2 lists the main properties of the three kinds of basic fuels; Table 3 lists the components and main properties of the blending fuels.

### **2.4. Operation conditions and procedure overview**

After a 15 minutes warm-up, the engine speed was adjusted to 1600 rpm and hold-onto. Without pilot-injection, about 25.25 mg fuel was injected into the cylinder at 7 deg BTDC (Before Top Dead Center) per engine cycle at 120 MPa injection pressure, and the brake mean effective pressure was 0.8 MPa (about 40% engine load) during the whole engine test. The other important parameters, i.e., intake pressure, intake temperature, and cooling water temperature were kept constant at 1.4 bar, 30±2 °C, and 85±3 °C, respectively. To get a detailed investigation of the influence of EGR rate on the engine performance and emission level in the multi-cylinder single injection CI engine with diesel/n-butanol/PODE<sub>3-4</sub> blending fuels, an EGR sweep (from 0 to 40%) was performed. Table 4 lists the detailed engine operation conditions.

## **3. Test data and discussions**

### **3.1 Impact of EGR rate on engine performances of blends regarding low-temperature combustion**

Figure 2 compares the curves of cylinder pressure and heat release rate for the four fuels at varied EGR rates. When blending diesel with n-butanol, peak values of both the cylinder pressure and the heat release rate rise, and the starting point of heat release is delayed. The main reason is that n-butanol has a relatively low cetane

number while the latent heat of evaporation is relatively large; the delayed ignition time delays the blending between fuel and air, so that more homogeneous blended mixture can form. Thus, the ratio of premixed combustion increases and peaks of both the heat release and the cylinder pressure rise. When blending BD20 with PODE<sub>3-4</sub>, PODE<sub>3-4</sub> may advance the heat release starting point, the peak value of heat release moves forward, and the peak of mean cylinder pressure rises. PODE<sub>3-4</sub> has higher cetane number and volatility than n-butanol; therefore, adding PODE<sub>3-4</sub> to BD20 increases the cetane number of the blend, enhances the quality of air-fuel mixture, shortens the ignition delay, and brings forward the starting point of combustion heat release and the peak of heat release. After adding PODE, the combustion chemical reaction rate grows, more fuel burns per unit of time, and the mean cylinder pressure becomes relatively large. Compared with n-butanol, the decline of cylinder pressure due to the piston down-stroke at a large EGR rate can be avoided.

Figure 3(a) compares the ignition delay of the four fuels at varied EGR rates. Multiple factors, such as compression temperature and pressure in engine operation, as well as fuel characteristics, can affect the ignition delay. As the EGR rate grows, both the cylinder pressure and temperature reduce, inducing a delay in the starting point of heat release and extending the ignition delay. Due to the large evaporative latent heat of n-butanol, the fuel absorbs a significant amount of heat during evaporation, so that the temperature in cylinder reduces. Meanwhile, n-butanol has the lowest cetane number while its self-ignition point is high; this delays the starting point of heat release, and therefore the ignition delay of BD20 is the longest. Moreover, PODE<sub>3-4</sub> has high cetane number; the addition of PODE<sub>3-4</sub> shortens the ignition delay, and as the proportion of PODE<sub>3-4</sub> grows, the ignition delay further reduces.

Figure 3(b) shows the maximum pressure rise rates of the four fuels at varied EGR rate. As the EGR rate grows, the maximum pressure rise rate reduces because as EGR rate grows, intake oxygen concentration declines, and the combustion chemical reaction rate of the fuel reduces. At a relatively small EGR rate (<25%), BD20 has the highest MPRR. The low cetane number of n-butanol, together with a long ignition



172 delay, increases the homogeneous mixture gas formed before the ignition, and  
173 increases the ratio of premixed combustion. When blending BD20 with PODE<sub>3-4</sub>, the  
174 ignitability of fuel improves, the ignition delay shortens, the ratio of premixed  
175 combustion reduces, and therefore the maximum pressure rise rate declines. When the  
176 EGR rate further grows, the delay of the ignition time is too long; then the piston  
177 descends to the lowest level and the volume of the combustion chamber thus enlarges,  
178 so the pressure rise rate drops sharply.

179 Figure 3(c) shows the relationship between combustion durations and EGR rates. The  
180 physicochemical properties of the fuel, ambient temperature, and ambient pressure  
181 affect the duration of combustion. From the figure, blending diesel with n-butanol can  
182 reduce the combustion duration because of the relatively high volatility of n-butanol  
183 that would ease the mixing of fuel and air, while the oxygen in the n-butanol molecule  
184 can facilitate the combustion. Because of the even better volatility and higher  
185 flammability of PODE<sub>3-4</sub>, adding PODE<sub>3-4</sub> to BD20 may increase the fuel-air mixing  
186 rate and the chemical reaction rate, and the combustion duration further reduces.

187 Figure 3(d) shows the relationship between brake thermal efficiencies at varied EGR  
188 rates. The brake thermal efficiency reduces with the growth of the EGR rate. As EGR  
189 rate grows, the inert gas content in cylinder rises, the fresh charging amount reduces,  
190 the cylinder combustion temperature declines, so the combustion heat release process  
191 of fuel is hindered, and the center of combustion is far away from the top dead center  
192 (TDC). At medium or small EGR rate (0-30%), due to the oxygen content in the n-  
193 butanol molecule and its good volatility, the brake thermal efficiency of BD20 is  
194 better than that of D100. Furthermore, the oxygen content is greater, the volatility is  
195 better, and the flammability is higher than that of BD20; therefore, brake thermal  
196 efficiencies of BDP10 and BDP20 further increase. When EGR rate further grows, the  
197 thermal efficiency of blends slightly differs from that of pure diesel because the  
198 excess air coefficient is too low at a large EGR rate, and EGR rate affects the thermal  
199 efficiency far more than the different fuel properties.

200 Figure 3(e) shows the changes in the relationship among the combustion efficiencies

and EGR rates. For medium or low EGR rate (0-30%), as the EGR rate grows, there is no significant difference in the combustion efficiencies and they keep relatively high values. When EGR rate further grows (>30%), the combustion efficiency drastically drops. because at medium or low EGR rate, the fuels have very small emissions of soot, CO, and HC (see Figs. 4(b)-4(d)); the combustion losses reduce, so the combustion efficiencies keep high. At large EGR rate, the emissions drastically rise (see Figs. 4(b)-4(d)) and this may deteriorate the combustion. Because of the highest emissions of CO and HC of BD20, it has the lowest combustion efficiency. After adding PODE<sub>3-4</sub> to BD20, the combustion efficiency gets better, and the combustion efficiency rises with the increase of the proportion of PODE<sub>3-4</sub>. Figure 3(f) shows the changes in the relationship between brake specific fuel consumptions and EGR rates. Increased EGR rate results in increased residual gas in the cylinder, deteriorated combustion and thus increased brake specific fuel consumption. Because the heat value is lower in the n-butanol than diesel, BD20 has a higher brake specific fuel consumption. Besides, the heat amount of PODE<sub>3-4</sub> is even lower than that of n-butanol, so the brake specific fuel consumption is further increased by adding PODE<sub>3-4</sub> to BD20.

### **3.2 Impact of EGR rate on regular emission characteristics of blends regarding low-temperature combustion**

Figure 4(a) and Figure 4(b) show the emissions of NO<sub>x</sub> and soot of four fuels at varied EGR rates. From the charts, at medium or low EGR rate (<30%), as the EGR rate grows, the emission of NO<sub>x</sub> significantly reduces while that of soot keeps relatively small. At relatively large EGR rate (>30%), as EGR rate grows, the emission of NO<sub>x</sub> keeps relatively low while that of soot drastically increases. In fact, at medium or low EGR rate, excess air coefficient in the cylinder is relatively large, so the oxygen content is adequate and the combustion temperature in cylinder is relatively high. This condition eases the oxidation of soot and generation of NO<sub>x</sub>; at relatively large EGR rates, the low excess air coefficient deteriorates the combustion increasing the emission of soot. At the same EGR rate, the high volatility of n-butanol

and PODE<sub>3-4</sub> can facilitate the mixing of fuel and air. Moreover, a high oxygen content can facilitate the combustion, so the emissions of NO<sub>x</sub> when using BD20, BDP10, and BDP20 are higher than those of D100, while that of soot is lower. At the EGR rate of 40%, compared with D100, the use of BD20 and BDP20 contributes to a reduction of soot emission about 44% and 62.7%, respectively.

Figure 4(c) and Figure 4(d) show the changes in the relationship between emissions of CO and HC of the four fuels at varied EGR rates. From Figure 4(c) and Figure 4(d), the variation law of CO emission at different EGR rates is similar to that of HC emission. At EGR rate <30%, the emissions of CO and HC keep relatively low; increasing the EGR rate (>30%), the emissions of CO and HC drastically rise. In fact, at medium or low EGR rate, the excess air coefficient in the cylinder is relatively large, the oxygen concentration is adequate, the excessively concentrated region in the cylinder decreases, and the combustion temperature is relatively high, thus easing the oxidation of CO and HC. When EGR rate further grows (>30%), the fresh charging amount reduces, inert gases increase, and the combustion temperature in the cylinder reduces preventing the oxidation of CO and HC. At relatively large EGR rate, n-butanol has low cetane number low, the ignition delay of BD20 is too long, and the fuel-air mixture is excessively diluted. Therefore, the high-temperature combustion process slows, combustion temperature reduces, and great amount of CO and HC generates. Because the high cetane value and high oxygen content that characterize PODE<sub>3-4</sub>, its addition to BD20 improves the flammability of BDP10 and BDP20. Therefore, the emissions of CO and HC significantly reduce.

### **3.3 Impact of EGR rate on particulate matter emission characteristics of blends regarding low-temperature combustion**

Figure 5 shows the change curves of particle size distributions for the four fuels at varied EGR rates. When the EGR rate is below 20%, the particulate matters mainly behave as nucleation particle distribution; above 30%, the particle size mainly manifests as accumulation particle size distribution. The main reason is that at small EGR rate, the high mean cylinder temperature is beneficial in oxidizing of large-size

particles into small-size nucleation particles so that the peak value of nucleation particle number concentration increases. Nevertheless, the further growth of EGR rate rapidly increases soot and HC (see Figs. 4(b) and 4(d)). Meanwhile, the volume of residual gases in the cylinder that contains multiple unburnt HC compounds, sulfates, and primary carbon particles increases, easing the rapid generation of accumulation particles.

Figure 6(a) shows the changes in the relationship between total particle number concentrations and EGR rates. As the EGR rate grows, the total particle number concentrations decline first and then rise, reaching their minimum values at the EGR rate of about 25%. Concerning EGR rate within the 0-25% range, as the EGR rate grows, the reduction of the peak values of nucleation particle number concentration results in the decline of total particle number concentrations. When EGR rate further grows, the increase of peak values of accumulation particle number concentration causes the total particle number concentrations rise.

Figure 6(b) shows the changes in the relationship between total particle mass concentrations and EGR rates. As EGR rate grows, the trends of total particle mass concentrations of the fuels are similar to those of soot emissions, keeping stable at first and then rising rapidly. The reason is that particle number and particle size determine the total particle mass concentration; the greater the number and the larger, the greater the total particle mass concentration. At small EGR rate, the nucleation particle number concentration is relatively high, but has small size (see Fig. 7), so the largest particles mainly affect the total particle mass concentration.

Figure 7 shows the changes in the relationship between geometric mean particle diameters of four different fuels at varied EGR rates. As the EGR rate grows, the geometric mean particle diameters of the fuels vary slowly at first and then rise rapidly. In fact, at large EGR rate, the insufficient oxygen concentration deteriorates the combustion, and carbon soot increases causing the increase of the biggest particles. When blending diesel with n-butanol, the particles geometric mean diameter reduces. Moreover, when adding PODE<sub>3-4</sub> to BD20 by 20%, the particles geometric

mean diameter further decreases because of the high volatility of PODE<sub>3-4</sub>; PODE<sub>3-4</sub> is beneficial to well mixing of fuel and air, and thus more homogeneous mixture is formed; at the same time, the oxygen content in n-butanol and PODE<sub>3-4</sub> molecules can facilitate the oxidation of large-size particles into small-size particles.

Figure 8 shows the changes in the relationship between the number concentrations of nucleation particle and accumulation particle of four fuels at varied EGR rates. The nucleation particle number concentrations drop rapidly at first and then tend to flatten with the growth of the EGR rate, while the accumulation particle number concentrations vary slightly at first and then rise rapidly. The main reason is that as the EGR rate grows, the cylinder temperature declines, which restrains the generation of nucleation particles and facilitates the increase of accumulation particle number. At small EGR rate, diesel blended with n-butanol can reduce the nucleation particle number concentrations. PODE<sub>3-4</sub> is added to the blend with BD20 by 10%, Because its high volatility and high oxygen content, PODE<sub>3-4</sub> can help in improving the anoxic situation of blends in the locally excessively concentrated regions, reducing the emissions of fine HC particles and precursors of nucleation particles, and further decreasing nucleation particle number concentrations. When blending fuel with 20% PODE<sub>3-4</sub>, the oxygen content concentration is even higher in the fuel, which is beneficial in the oxidation of large-size particles in late combustion stage, causing the growth of the number of small-size particles and nucleation particle number concentrations. However, the effect of the blend on accumulation particle number concentration is not significant.

Figure 9 shows the particulate number concentrations for various diameter ranges at various EGR rates. From the figures, at medium or low EGR rates (<20%) small-size particles (sub-50nm) dominate the emission of particles, whereas the effect of accumulation particles (see Fig. 5) prevails at large EGR rates (>30%). Figure 10 shows the ratio of small-size particle (sub-25nm) number concentration to total number concentration for each of the fuels. At the EGR rate of 0% or 20%, the ratio of the small-size particle (sub-25nm) number concentration to total particle number

concentration is very large. At the EGR rate of 30% or 40%, the ratio of small-size particle number concentration to total particle number concentration significantly reduces because at medium or low EGR rates the emissions of soot and HC are low (see Fig. 4(b) and Fig. 4(d)), and the high oxygen concentration boosts the oxidation of large-size particles during the combustion. Consequently, the ratio of small-size particle number concentration increases. At large EGR rates, the emissions of soot and HC deteriorate (see Fig. 4(b) and Fig. 4(d)) and the in-cylinder temperature also reduces, which restrains the oxidation of large-size particles (see Fig. 9).

#### 4. Conclusions

This study mainly investigates the combustion and emission characteristics of four fuels (D100, BD20, BDP10, and BDP20) regarding the low-temperature combustion mode of a CI engine at varied EGR rates under medium engine loads. The following conclusions can be drawn.

1. At the same EGR rate, the comparison between D100 and BD20 fuels highlights that, for BD20, the peak values of mean cylinder pressure and heat release rate increase, ignition delay is extended, and combustion efficiency reduces. When adding PODE<sub>3-4</sub> to BD20, the ignition delay shortens, the peak values of heat release and mean cylinder pressure rise, the brake thermal efficiency and the combustion efficiency increase, and the specific fuel consumption rises.

2. At EGR rate lower than 30%, as the EGR rate grows, the effects on the emissions of soot, CO, and HC are not significant, while the emission of NO<sub>x</sub> drops sharply. Moreover, at EGR rate larger than 30%, as the EGR rate grows, the emissions of soot, CO, and HC rise rapidly. Compared with D100, for BD20 the emissions of CO, HC, and NO<sub>x</sub> rise, while that of soot decreases significantly. Finally, when adding PODE<sub>3-4</sub> to BD20, the emissions of soot, CO, and HC decline.

3. As EGR rate grows, the total particulate number concentrations of the four fuels decline at first and then rise, the total particle mass concentrations keep stable at first and then increase sharply, and the geometric mean diameters of particles change

slowly at first and then rise rapidly. Compared with D100, the peak value of the nucleation particle number concentration of BD20 declines and the geometric mean diameter of particles reduces. The addition of POE<sub>3-4</sub> to BD20 causes the peak value of the concentration of nucleation particle number decline at first and then rise, while the geometric mean diameter of particles further reduces. At medium or low EGR rate, the ratio of small-size particle (sub-25 nm) number concentration to total particle number concentration is significant for each of the four fuels. At large EGR rate, the ratio of small-size particle (sub-25 nm) number concentration to total particle number concentration reduces significantly.

## **5. Acknowledgement**

The research is sponsored by projects of Natural Science Foundation of Guangxi (project Outstanding Young Scholarship Award, Grant No.2014GXNSFGA118005), Natural Science Foundation of China (Grant No.51076033), and Guangxi Science and Technology Development Plan (AC16380047).

## **6. Reference**

- [1] Srihari S, Thirumalini S, Prashanth K, et al. An experimental study on the performance and emission characteristics of PCCI-DI engine fuelled with diethyl ether-biodiesel-diesel blends. *Renewable Energy* 2017, 107:440-447.
- [2] Poorghasemi K, Saray R K, Ansari E, et al. Effect of diesel injection strategies on natural gas/diesel RCCI combustion characteristics in a light duty diesel engine. *Applied Energy* 2017, 199.
- [3] Pinazzi P M, Foucher F. Influence of injection parameters, ozone seeding and residual NO on a Gasoline Compression Ignition (GCI) engine at low load. *Proceedings of the Combustion Institute* 2016.
- [4] Shi L, Xiao W, Li M, et al. Research on the Effects of Injection Strategy on LTC Combustion based on Two-Stage Fuel Injection. *Energy* 2017, 121.

- 371 [5] Zaharin M S M, Abdullah N R, Najafi G, et al. Effects of physicochemical  
372 properties of biodiesel fuel blends with alcohol on diesel engine performance and  
373 exhaust emissions: A review. *Renewable & Sustainable Energy Reviews* 2017,  
374 79:475-493.
- 375 [6] Yusri I M, Mamat R, Najafi G, et al. Alcohol based automotive fuels from  
376 first four alcohol family in compression and spark ignition engine: A review on  
377 engine performance and exhaust emissions. *Renewable & Sustainable Energy*  
378 *Reviews* 2017, 77:169-181.
- 379 [7] Jamrozik A. The effect of the alcohol content in the fuel mixture on the  
380 performance and emissions of a direct injection diesel engine fueled with diesel-  
381 methanol and diesel-ethanol blends. *Energy Conversion & Management* 2017,  
382 148:461-476.
- 383 [8] Krishnamoorthi M, Malayalamurthi R. Experimental investigation on  
384 performance, emission behavior and exergy analysis of a variable compression  
385 ratio engine fueled with diesel - aeglemarmelos oil - diethyl ether blends. *Energy*  
386 2017, 128:312-328.
- 387 [9] Ibrahim A. Investigating the effect of using diethyl ether as a fuel additive on  
388 diesel engine performance and combustion. *Applied Thermal Engineering* 2016,  
389 107:853-862.
- 390 [10] KapuraTudu, S. Murugan, S.K. Patel. Effect of diethyl ether in a DI diesel  
391 engine run on a tyre derived fuel-diesel blend. *Journal of the Energy Institute*  
392 2016, 89(4):525-535.
- 393 [11] Saleh H E, Selim M Y E. Improving the performance and emission  
394 characteristics of a diesel engine fueled by jojoba methyl ester-diesel-ethanol  
395 ternary blends. *Fuel* 2017.
- 396 [12] Gad M S, El-Araby R, Abed K A, et al. Performance and emissions  
397 characteristics of C.I. engine fueled with palm oil/palm oil methyl ester blended



398 with diesel fuel. Egyptian Journal of Petroleum 2017.

399 [13] Kaimal V K, Vijayabalan P. A detailed investigation of the combustion  
400 characteristics of a DI diesel engine fuelled with plastic oil and rice bran methyl  
401 ester. Journal of the Energy Institute 2017, 90(2):324-330.

402 [14] Johnson D, Heltzel R, Nix A, et al. Greenhouse gas emissions and fuel  
403 efficiency of in-use high horsepower diesel, dual fuel, and natural gas engines for  
404 unconventional well development. Applied Energy 2017, 206:739-750.

405 [15] Yang B, Ning L, Chen W H, et al. Parametric investigation the particle  
406 number and mass distributions characteristics in a diesel/natural gas dual-fuel  
407 engine. Applied Thermal Engineering 2017.

408 [16] Algayyim, SattarJabbarMurad, Wandel, et al. The impact of n-butanol and  
409 iso-butanol as components of butanol-acetone (BA) mixture-diesel blend on  
410 spray, combustion characteristics, engine performance and emission in direct  
411 injection diesel engine. Energy 2017.

412 [17] Han X, Yang Z, Wang M, et al. Clean combustion of n -butanol as a next  
413 generation biofuel for diesel engines. Applied Energy 2016, 198.

414 [18] MdNurunNabi, Ali Zare, Farhad M. Hossain, et al. A parametric study on  
415 engine performance and emissions with neat diesel and diesel-butanol blends in  
416 the 13-Mode European Stationary Cycle. Energy Conversion and Management  
417 2017, 148:251-259.

418 [19] Pereira L G, Dias M O S, Mariano A P, et al. Economic and environmental  
419 assessment of n-butanol production in an integrated first and second generation  
420 sugarcane biorefinery: Fermentative versus catalytic routes. Applied Energy  
421 2015, 160:120-131.

422 [20] Ndaba B, Chiyanzu I, Marx S. n-Butanol derived from biochemical and  
423 chemical routes: A review: Biotechnology Reports 2015, 8(C):1-9.

- 424 [21] Yue W, Ho S H, Yen H W, et al. Current advances on fermentative  
425 biobutanol production using third generation feedstock. *Biotechnology Advances*  
426 2017.
- 427 [22] Jin C, Yao M, Liu H, et al. Progress in the production and application of n-  
428 butanol as a biofuel. *Renewable & Sustainable Energy Reviews* 2011,  
429 15(8):4080-4106.
- 430 [23] Dernet J, Mounaïm-Rousselle C, Halter F, et al. Evaluation of Butanol-  
431 Gasoline Blends in a Port Fuel-injection, Spark-Ignition Engine. *Oil & Gas*  
432 *Science & Technology* 2009, 65(2):345-351.
- 433 [24] Cheng X, Li S, Yang J, et al. Investigation into partially premixed  
434 combustion fueled with N-butanol-diesel blends. *Renewable Energy*  
435 2016;86:723–32.
- 436 [25] Huang H, Zhou C, Liu Q, et al. An experimental study on the combustion  
437 and emission characteristics of a diesel engine under low temperature combustion  
438 of diesel/gasoline/n-butanol blends. *Applied Energy* 2016, 170:219-231.
- 439 [26] Huang H, Liu Q, Yang R, et al. Investigation on the effects of pilot injection  
440 on low temperature combustion in high-speed diesel engine fueled with n-  
441 butanol–diesel blends. *Energy Conversion & Management* 2015, 106:748-758.
- 442 [27] Zhang Z H, Balasubramanian R. Influence of butanol–diesel blends on  
443 particulate emissions of a non-road diesel engine. *Fuel* 2014, 118(118):130-136.
- 444 [28] Li D, Gao Y, Liu S, et al. Effect of polyoxymethylene dimethyl ethers  
445 addition on spray and atomization characteristics using a common rail diesel  
446 injection system. *Fuel* 2016, 186:235-247.
- 447 [29] Zheng Y, Tang Q, Wang T, et al. Kinetics of synthesis of polyoxymethylene  
448 dimethyl ethers from paraformaldehyde and dimethoxymethane catalyzed by ion-  
449 exchange resin. *Chemical Engineering Science* 2015, 134:758-766.

450 [30] Liu H, Wang Z, Wang J, et al. Improvement of emission characteristics and  
451 thermal efficiency in diesel engines by fueling gasoline/diesel/PODEn blends.  
452 Energy 2016, 97:105-112.

453 [31] Liu H, Wang Z, Wang J, et al. Performance, combustion and emission  
454 characteristics of a diesel engine fueled with polyoxymethylene dimethyl ethers  
455 (PODE<sub>3-4</sub>)/diesel blends. Energy 2015, 88:793-800.

456 [32] Liu H, Ma X, Li B, et al. Combustion and emission characteristics of a direct  
457 injection diesel engine fueled with biodiesel and PODE/biodiesel fuel blends.  
458 Fuel 2017, 209:62-68.

459 [33] Huang H, Teng W, Li Z, et al. Improvement of emission characteristics and  
460 maximum pressure rise rate of diesel engines fueled with n-butanol/PODE<sub>3-4</sub>  
461 /diesel blends at high injection pressure. Energy Conversion & Management  
462 2017, 152:45-56.

463 [34] Liu H, Wang Z, Li B, et al. Exploiting new combustion regime using  
464 multiple premixed compression ignition (MPCI) fueled with  
465 gasoline/diesel/PODE (GDP). Fuel 2016, 186:639-647.

466 [35] Tong L, Wang H, Zheng Z, et al. Experimental study of RCCI combustion  
467 and load extension in a compression ignition engine fueled with gasoline and  
468 PODE. Fuel 2016, 181:878-886.

469 [36] Li B, Li Y, Liu H, et al. Combustion and emission characteristics of diesel  
470 engine fueled with biodiesel/PODE blends. Applied Energy 2017, 206:425-431.

471 [37] Liu J, Wang H, Li Y, et al. Effects of diesel/PODE (polyoxymethylene  
472 dimethyl ethers) blends on combustion and emission characteristics in a heavy  
473 duty diesel engine. Fuel 2016, 177:206-216.

474 [38] Liu J, Sun P, Huang H, et al. Experimental investigation on performance,  
475 combustion and emission characteristics of a common-rail diesel engine fueled  
476 with polyoxymethylene dimethyl ethers-diesel blends. Applied Energy 2017, 202.

- 477 [39] Huang H, Liu Q, Teng W, et al. Improvement of combustion performance  
478 and emissions in diesel engines by fueling n -butanol/diesel/PODE<sub>3-4</sub>, mixtures.  
479 Applied Energy 2017.
- 480 [40] Zhang Q, Yao M, Zheng Z, et al. Experimental study of n-butanol addition  
481 on performance and emissions with diesel low temperature combustion.  
482 Energy 2012;47(1):515–21.

1    **Tables**

2    **Table 1** Technical specifications of test engine.

3    **Table 2** Detail physical and chemical properties of test fuels.

4    **Table 3** Component of blend fuels.

5    **Table 4** Operating conditions of engine.

6   **Figures**

7   **Fig. 1** Schematic diagram of the experimental system

8   **Fig. 2** Curves of mean cylinder pressure and heat release rate of four different fuels at  
9   varied EGR rates

10   **Fig. 3** Combustion characteristics and fuel consumption of four different fuels at  
11   varied EGR rates

12   **Fig. 4** Regular emission characteristics of four different fuels at varied EGR rates

13   **Fig. 5** Particle size distribution of four fuels with varied EGR rates

14   **Fig. 6** Total particle number and mass concentration of four different fuels at varied  
15   EGR rates

16   **Fig. 7** Geometric mean diameter of the four different fuels at varied EGR rates

17   **Fig. 8** Nucleation particle and accumulation particle number concentration of the four  
18   different fuels at varied EGR rates

19   **Fig. 9** Particle number concentration of four fuels for various diameter ranges at  
20   varied EGR rates

21   **Fig. 10** The particulate mass number concentration of the four different fuels at varied  
22   EGR rates

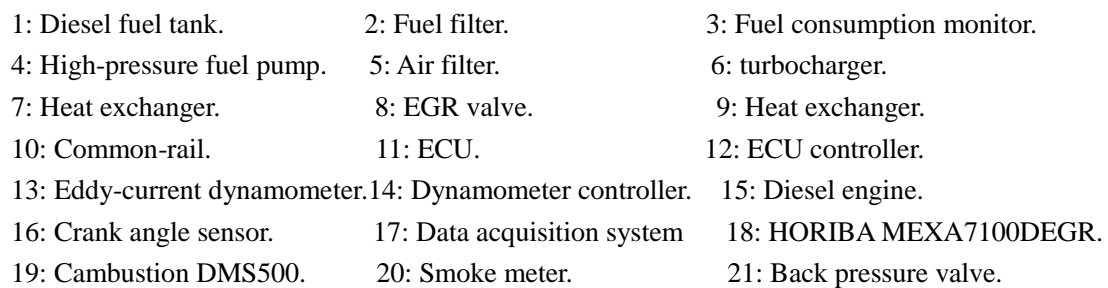


Fig. 1. Schematic diagram of the experimental system.

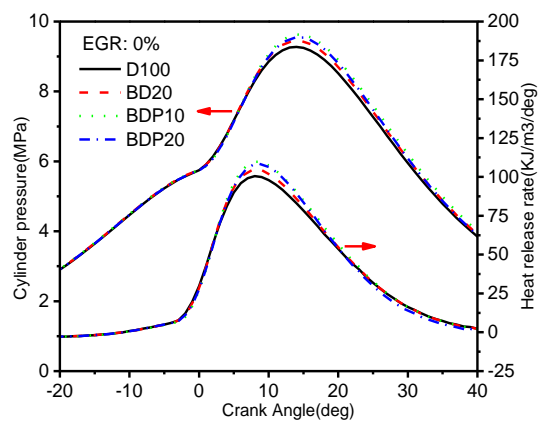


Fig. 2(a) EGR: 0%

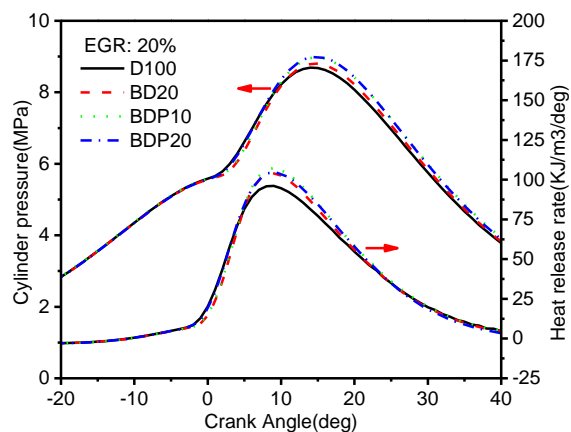


Fig. 2(b) EGR: 20%

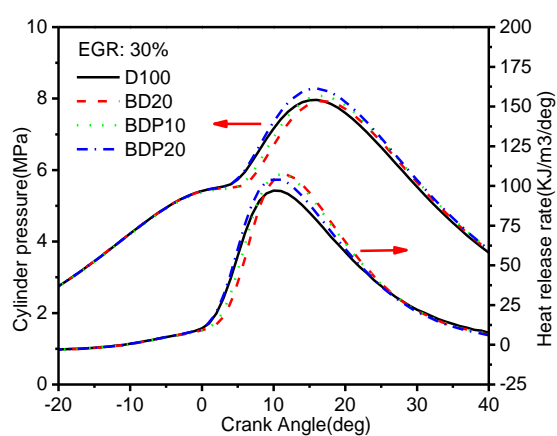


Fig. 2(c) EGR: 30%

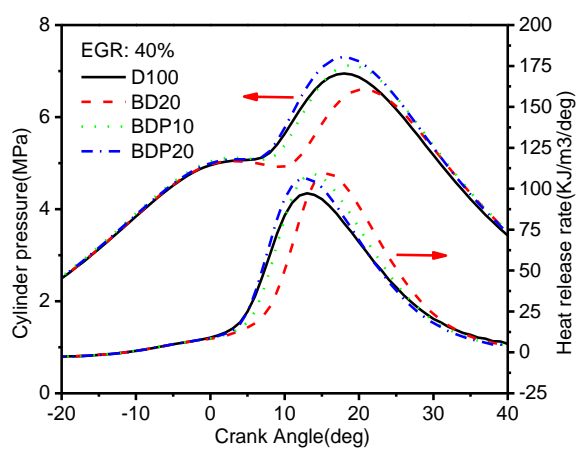


Fig. 2(d) EGR: 40%

Fig. 2. Curves of mean cylinder pressure and heat release rate of four different fuels at varied EGR rates



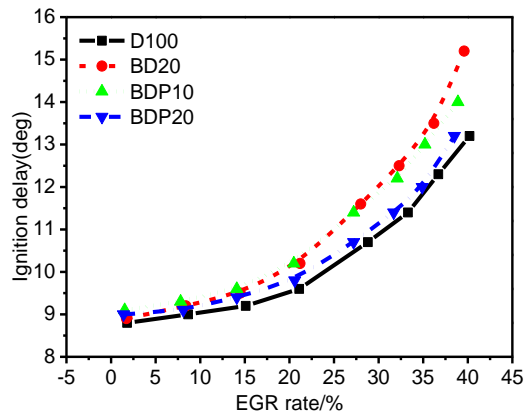


Fig.3(a) Ignition delay

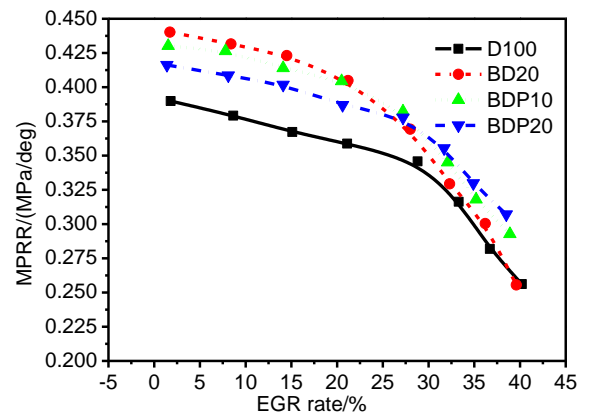


Fig.3(b) Maximum pressure rise rate

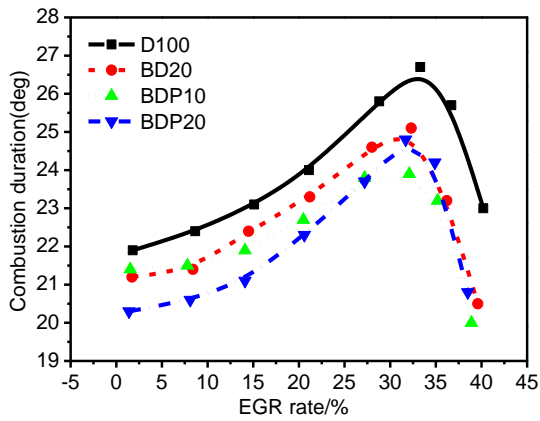


Fig.3(c) Combustion duration

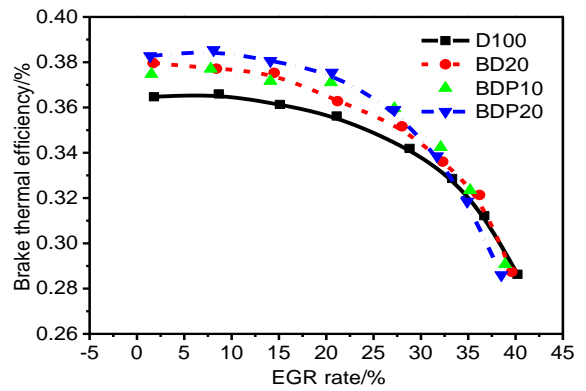


Fig.3(d) Brake thermal efficiency

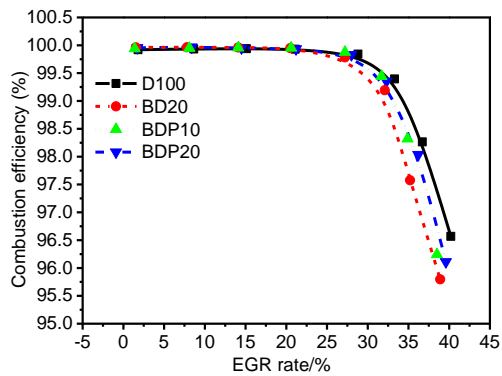


Fig.3(e) Combustion efficiency

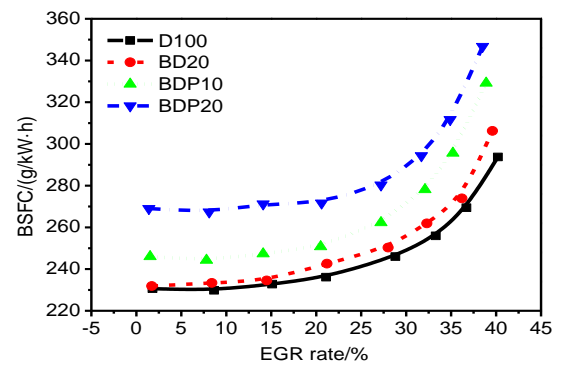


Fig.3(f) The brake specific fuel consumption

Fig.3. Combustion characteristics and fuel consumption of four different fuels at varied EGR rates

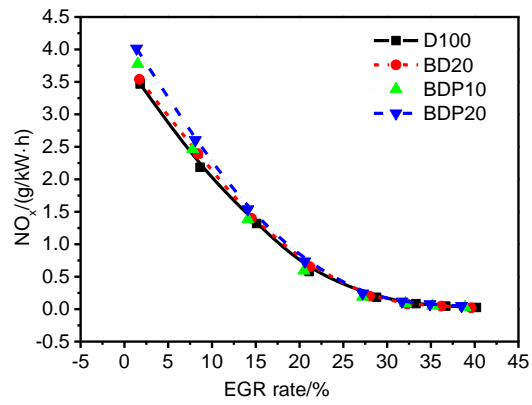


Fig.4(a) NOx emission

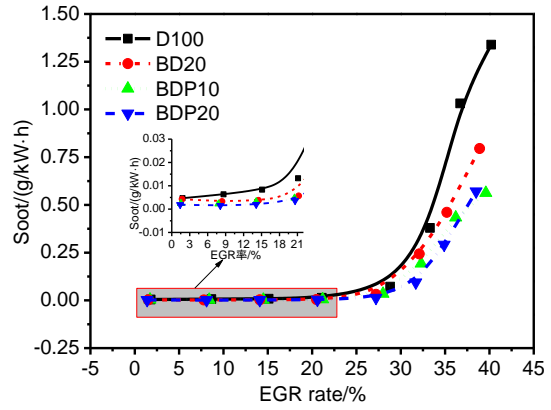


Fig.4(b) Soot emission

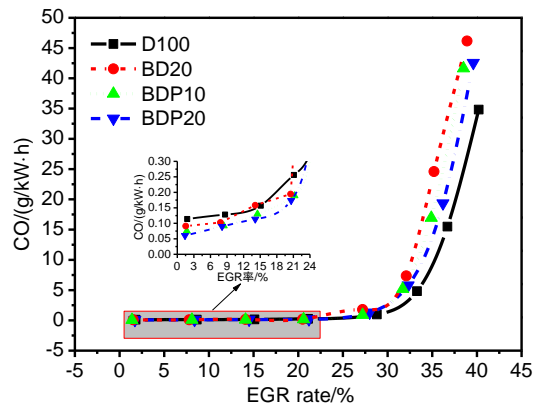


Fig.4(c) CO emission

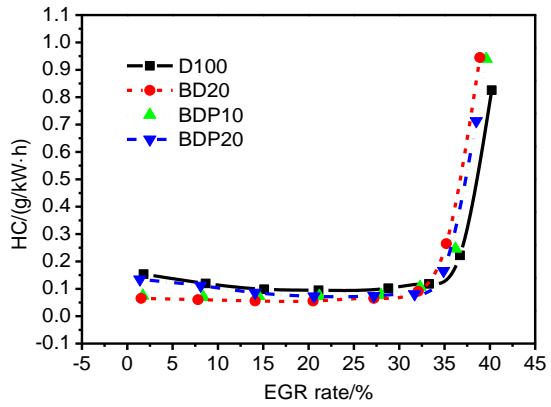


Fig.4(d) HC emission

Fig.4. Regular emission characteristics of four different fuels at varied EGR rates

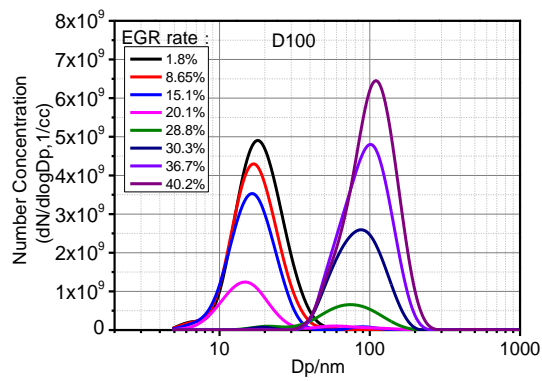


Fig.5(a) D100

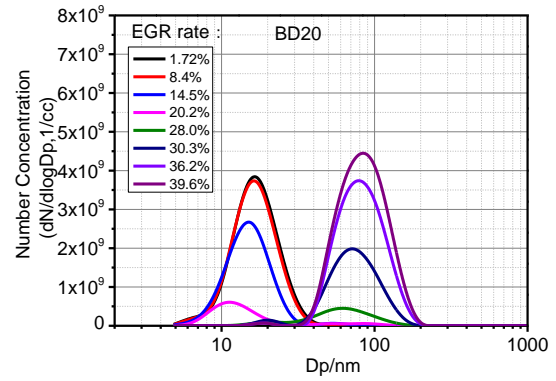


Fig.5(b) BD20

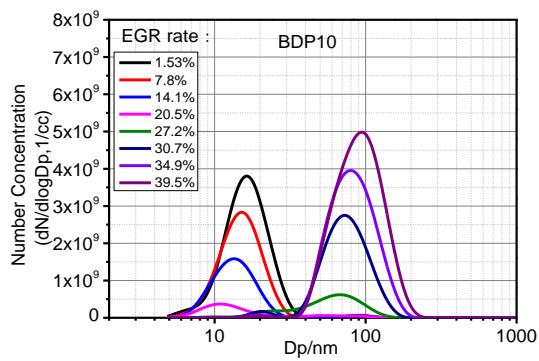


Fig.5(c) BDP10

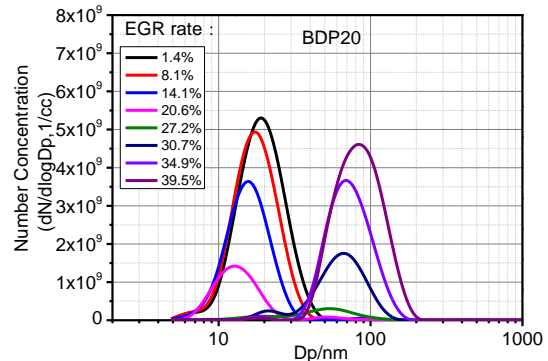


Fig.5(d) BDP20

Fig.5. Particle size distribution of four fuels with varied EGR rates

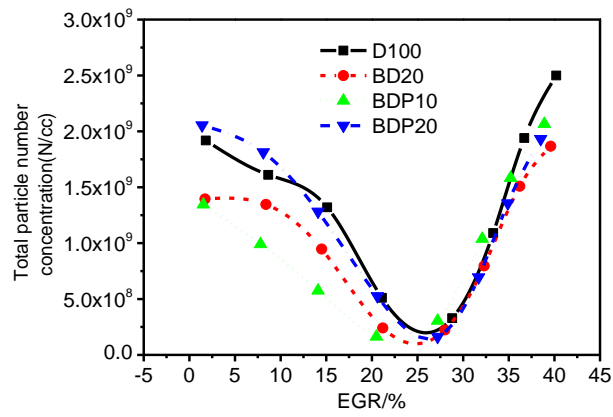


Fig.6(a) Total particle number concentration

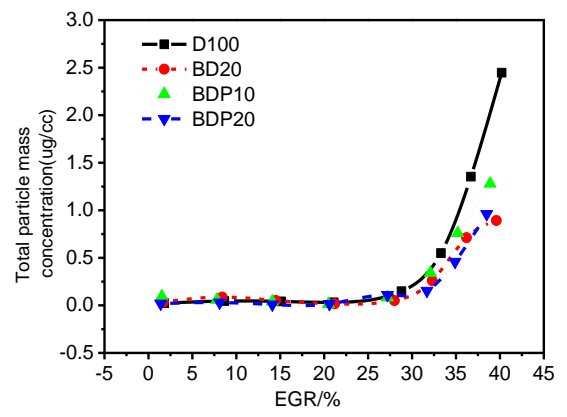


Fig.6(b) Total particle mass concentration

Fig.6. Total particle number and mass concentration of four different fuels at varied EGR rates

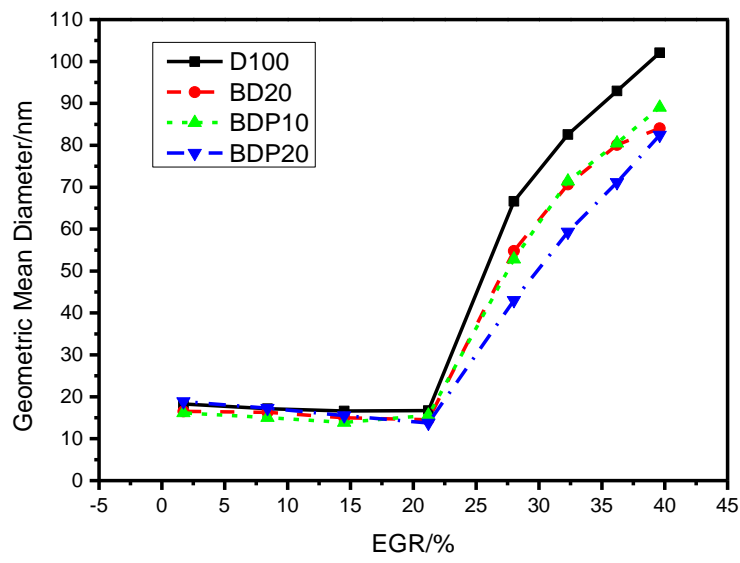


Fig.7. Geometric mean diameter of the four different fuels at varied EGR rates

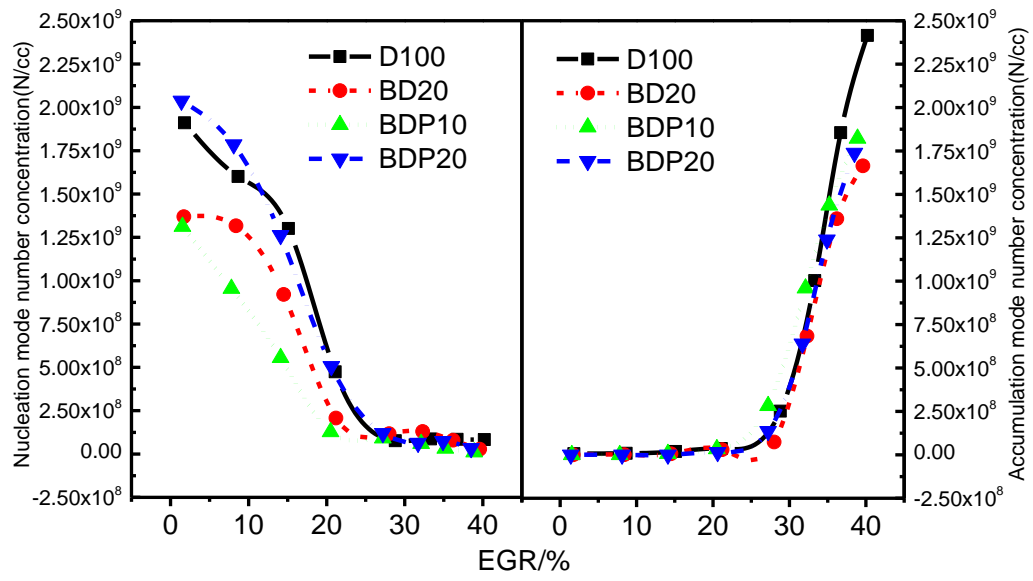


Fig. 8. Nucleation particle and accumulation particle number concentration of the four different fuels at varied EGR rates

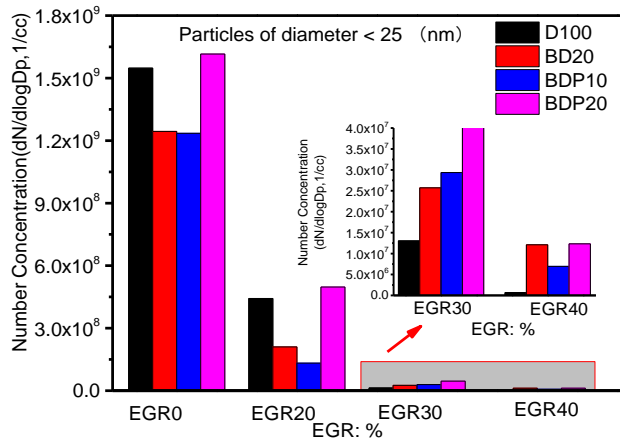


Fig. 9(a) Particle number concentration of different fuels varying the EGR rates (diameter<25 (nm))

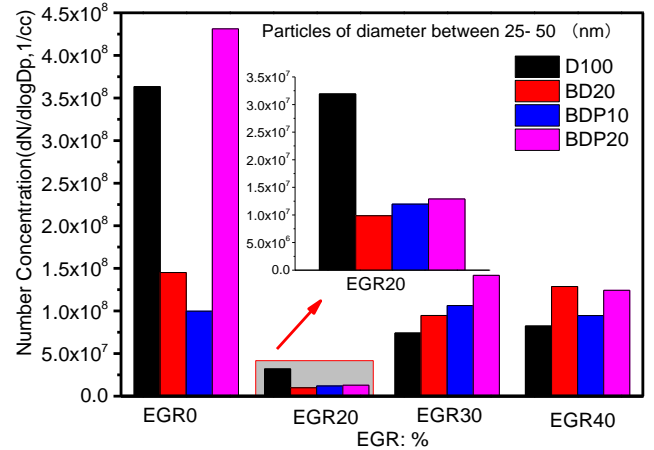


Fig. 9(b) Particle number concentration of different fuels varying the EGR rates(25(nm)<diameter<50(nm))

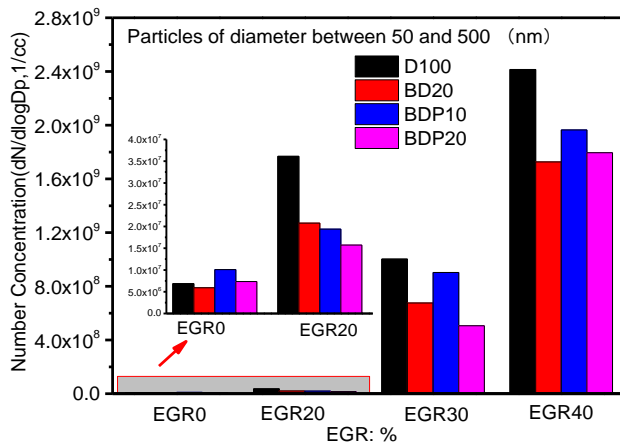


Fig. 9(c) Particle number concentration of the four different fuels varying the EGR rates (50 (nm) <diameter<500 (nm) )

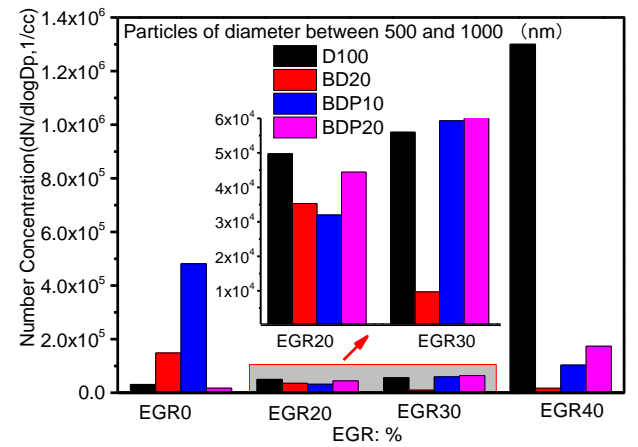


Fig. 9(d) Particle number concentration of the four different fuels varying the EGR rates (500 (nm) <diameter<1000 (nm) )

Fig. 9. Particle number concentration of four fuels for various diameter ranges at varied EGR rates

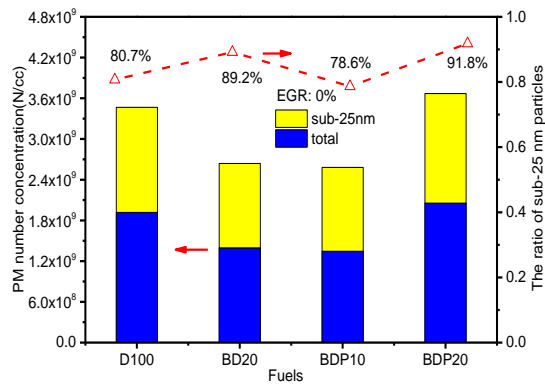


Fig. 10(a) Particulate mass number concentration of the four different fuels; EGR of 0%

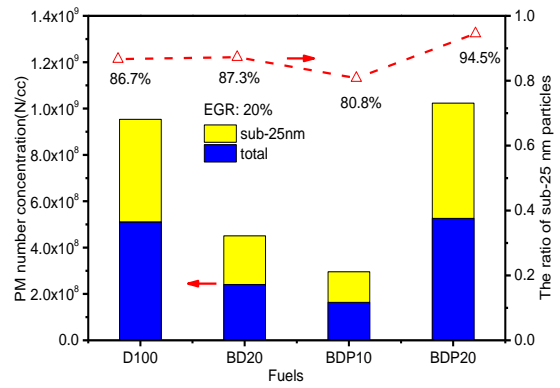


Fig. 10(b) Particulate mass number concentration of the four different fuels. EGR of 20%

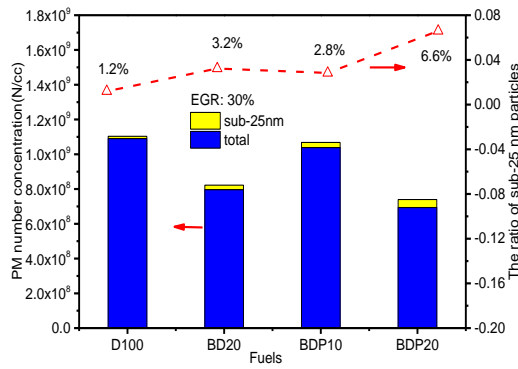


Fig. 10(c) Particulate mass number concentration of the four different fuels. EGR of 30%

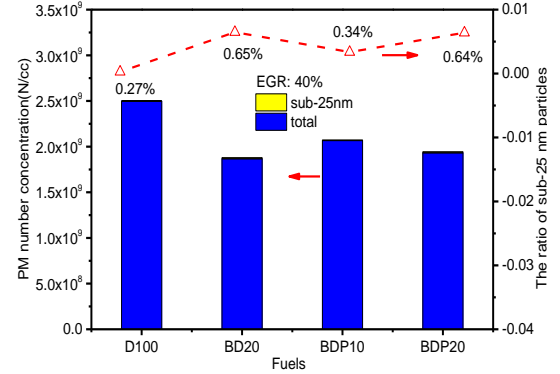


Fig. 10(d) Particulate mass number concentration of the four different fuels. EGR of 40%

Fig. 10. The particulate mass number concentration of the four different fuels at varied EGR rates



**Table 1** Technical specifications of test engine.

Item	value
Number of cylinders	4
Cylinder diameter(mm)	85
Number of valves	16
Stroke (mm)	88.1
Displacement (L)	1.99
Maximum torque (N.m)	286
Compression ratio	16.5
Rated power (kW)/speed (r/min)	100/4000

.

**Table 2** Detail physical and chemical properties of test fuels.

	Diesel <sup>a</sup>	n-butanol <sup>b</sup>	PODE <sub>3-4</sub> <sup>c</sup>
Molecular formula	C <sub>12</sub> -C <sub>25</sub>	C <sub>4</sub> H <sub>10</sub> O	CH <sub>3</sub> O(CH <sub>2</sub> O) <sub>n</sub> CH <sub>3</sub>
Cetane number	54	17	78.4
Research octane number	-	96	-
Oxygen content (%)	-	21.62	46.98
Density (g /mL)	0.82	0.81	1.019
Low heat value (MJ /kg)	42.8	33.2	19.05
Boiling point (°C)	180-360	117	156.202
Kinematic viscosity (mm <sup>2</sup> . s-1 @20 °C)	4.8	3.64	1.05

<sup>a</sup> Source: ASTM D975.

<sup>b</sup> Source: Name [40].

<sup>c</sup> Source: Name [31].

23 **Table 3** Component of blend fuels.

	Component volume percentage			Cetane number
	diesel	n-butanol	PODE <sub>3-4</sub>	
D100	100	0	0	54
BD20	80	20	0	45.4 <sup>a</sup>
BDP10	72	18	10	48.7 <sup>a</sup>
BDP20	64	16	20	52 <sup>a</sup>

<sup>a</sup> taken from Ref. [39]

**Table 4** Operating conditions of engine.

Item	Parameters
Speed (rpm)	1600
BMEP (MPa)	0.8 (45% load)
Fuel injection (mg/hug)	25.25
Injection pressure (MPa)	120
Injections	Single
Injection time ( °CA BTDC)	7
EGR ratio (%)	0-40%
Intake pressure (bar)	1.4
Intake temperature (°C)	30±2
Coolant temperature (°C)	85±3